Quantum Zeno switch for single-photon coherent transport

Lan Zhou (周兰),[1,2] S. Yang (杨硕),[3] Yu-xi Liu (刘玉玺),[2,4] C. P. Sun (孙昌璞),[3,2] and Franco Nori (野理)[2,4,5]
[1]*Department of Physics, Hunan Normal University, Changsha 410081, China*
[2]*Advanced Science Institute, The Institute of Physical and Chemical Research (RIKEN), Wako-shi 351-0198, Japan*
[3]*Institute of Theoretical Physics, The Chinese Academy of Sciences, Beijing 100080, China*
[4]*CREST, Japan Science and Technology Agency (JST), Kawaguchi, Saitama 332-0012, Japan*
[5]*Center for Theoretical Physics, Physics Department, Center for the Study of Complex Systems, The University of Michigan, Ann Arbor, Michigan 48109-1040, USA*

(Received 17 December 2008; published 11 December 2009)

Using a dynamical quantum Zeno effect, we propose a general approach to control the coupling between a two-level system (TLS) and its surroundings, by modulating the energy-level spacing of the TLS with a high-frequency signal. We show that the TLS-surroundings interaction can be turned off when the ratio between the amplitude and the frequency of the modulating field is adjusted to be a zero of a Bessel function. The quantum Zeno effect of the TLS can also be observed by the vanishing of the photon reflection at these zeros. Based on these results, we propose a quantum switch to control the transport of a single photon in a one-dimensional waveguide. Our analytical results agree well with numerical results using Floquet theory.

DOI: 10.1103/PhysRevA.80.062109 PACS number(s): 03.65.Xp, 32.80.Qk, 42.50.Dv, 03.67.Lx

I. INTRODUCTION

The quantum Zeno effect (QZE) [1] was once described as the quantum version of the expression "a watched pot never boils." Namely, an unstable particle, if observed constantly, will not decay [2–6]. This effect has been explained (e.g., Refs. [1,7,8]) in terms of wave-packet collapse: once a quantum measurement is performed, the superposed quantum state is reduced to a single one of the allowed eigenstates of the measured observable.

However, many authors (e.g., Refs. [9–15]) explained the QZE [16–18] *without* invoking the wave-function collapse. This *dynamical* QZE does not involve quantum states collapsing in one eigenstate and thus evolves in time. Indeed, Peres [9] argued that the decay of an unstable quantum system can be slowed down and even halted by its continual interaction with an external system, without measurement or observation. This dynamical QZE is sometimes called "bang-bang" control (e.g., in Refs. [13–15]). Here, we apply the dynamic QZE to realize a quantum switch.

The QZE can be used as a dynamical mechanism to suppress the environment-induced decoherence of a quantum system [7,15]. This implies that the coupling between the system and its environment can be controlled via the QZE. Here, we propose a quantum "Zeno switch" to turn on or off the quantum coherent transport of particles along a one-dimensional (1D) continuum.

A quantum switch [19–21] is regarded as an active device to control the transport of particles or the transfer of quantum states. It plays a similar role to the gate voltage, which turns on or off the transmission of electrons, in conventional electronic circuits. The quantum version of the switch means that the operations involve a single quantum. An example is the single-photon transistor [22–27], where the transport of a single photon in a 1D waveguide can be controlled by a two-level system (TLS) externally driven by a classical field.

A discrete-coordinate scattering approach [21] was developed to study a quantum switch for the coherent transport of a single photon along a 1D coupled-resonator waveguide (CRW). That quantum switch [21] can be realized by changing either the energy-level spacing or the coupling constants between the waveguide and a controller. Physical systems proposed to realize single-photon switches include (i) superconducting transmission line resonators coupled to a superconducting charge qubit [21] and (ii) a TLS coupled to a photonic crystal "defect-cavity" waveguide [20]. For the case (i), the controllability can be realized by changing the energy-level spacing of the charge qubit. However, it seems difficult to control well the photon transport in (ii) because the couplings and TLS parameters are fixed once the sample is fabricated [26,27].

In this paper, for a single photon propagating in a 1D CRW, a dynamical QZE switch is proposed with a tunable effective coupling to a TLS. This coupling is controlled by an applied frequency-modulated electromagnetic field. The photon can be transmitted either directly through the continuum, or indirectly, via a discrete energy level provided by the TLS. These two channels interfere with each other. Their destructive quantum interference prevents the photon transport while the constructive one leads to a total transmission [28]. The dynamic Zeno effect of the TLS could be actively controlled by a frequency modulation to switch between the two quantum interference channels. When the dynamic Zeno effect slows down the transitions in the TLS, the photon transport appears only when the TLS is in its ground state; no destructive quantum interference occurs. Then, effectively, the TLS and the continuum are decoupled.

II. DECOUPLING MECHANISM USING DYNAMICAL QZE

We generally consider a quantum system S with a characterized frequency ω_c and free Hamiltonian H_e, coupled to a TLS, with its ground $|g\rangle$ and excited $|e\rangle$ states, and energy-level spacing ω_a (with $\hbar=1$). We assume that a periodically modulated field is applied to TLS so that

$$\omega_a \to \Omega_a(t) = \omega_a + \Omega\cos(\nu t), \tag{1}$$

where Ω is the amplitude of the modulation with frequency ν. Hamiltonian

$$H = \Omega_a(t)|e\rangle\langle e| + G|e\rangle\langle g| + G^*|g\rangle\langle e| + H_e \tag{2}$$

describes the quantum system S and the TLS, as well as the coupling between them. The coupling coefficient G depends on S variables so that

$$e^{iH_e t}Ge^{-iH_e t} = Ge^{-i\omega_c t}. \tag{3}$$

In the interaction picture, the *coupling* between S and the TLS is modeled by the Hamiltonian

$$H_I = G\sum_{n=-\infty}^{+\infty} J_n\left(\frac{\Omega}{\nu}\right)e^{i(n\nu-\Delta)t}|e\rangle\langle g| + \text{H.c.}, \tag{4}$$

where the detuning $\Delta=\omega_c-\omega_a$. In Eq. (4), we have used [28] the Fourier-Bessel series identity,

$$e^{ix\sin\gamma} = \sum_n J_n(x)e^{in\gamma},$$

with the nth Bessel function $J_n(x)$ of the first kind.

For a fast modulation with large ν, the lowest-frequency terms in Eq. (4) dominate the dynamical evolution. These terms are determined by the near-resonant and resonant condition $(n\nu-\Delta)\simeq 0$; here $n=[\Delta/\nu]$ is the integer nearest to Δ/ν. To the lowest-frequency term of the index $n=[\Delta/\nu]$, Eq. (4) is approximated as

$$H_I \approx GJ_{[\Delta/\nu]}\left(\frac{\Omega}{\nu}\right)e^{(i[\Delta/\nu]\nu-\Delta)t}|e\rangle\langle g| + \text{H.c.} \tag{5}$$

For a very fast modulation of frequency ν (i.e., $\Delta/\nu\sim 0$) and a large Ω, we have

$$H_I \propto J_0(\Omega/\nu).$$

The values of the decoupling points (i.e., $\Omega/\nu \cong 2.40, 5.52, \ldots$) are just the zeros of $J_0(x)$. Equation (5) clearly shows that the *effective interaction vanishes* when the ratio Ω/ν (=amplitude/frequency of the driving field) is a zero of the Bessel function $J_{[\Delta/\nu]}(x)$, therefore, *decoupling* S from the TLS. At these zeros, the dynamical QZE occurs; namely, the TLS initially prepared in its excited state will remain there and will not decay to the ground state.

The above arguments to realize the QZE dynamics do not depend on the concrete form of the quantum system S. Thus, its based idea can be generally used for the various decoupling schemes.

Notice that the Bessel functions $J_n(x)$ look roughly like oscillating sine or cosine functions and have an infinite number of zeros. The decays of the Bessel functions are proportional to $1/\sqrt{x}$. Except asymptotically large x, the roots of the Bessel functions are not periodic.

III. SINGLE-PHOTON QUANTUM SWITCH IN A 1D WAVEGUIDE

Based on the above dynamical QZE mechanism, we now propose a quantum device, which behaves as a switch to control the incident photon transport in a CRW made of a periodic array of identical coupled resonators. The main difference between this device and the one in Ref. [21] is that here the TLS energy-level spacing is now modulated by a periodic field, allowing us to use the remarkable dynamic QZE in a very unusual manner. The 1D CRW is schematically shown in Fig. 1(a), where a TLS is embedded in one of the resonators and is modulated with the external periodic forcing of amplitude Ω and frequency ν, i.e., $\omega_a \to \Omega_a(t)$. Let $a_j^\dagger$ $(j=-\infty,\ldots,\infty)$ be the creation operator of the jth single mode cavity, all with the same frequency ω. The Hamiltonian of the CRW reads as

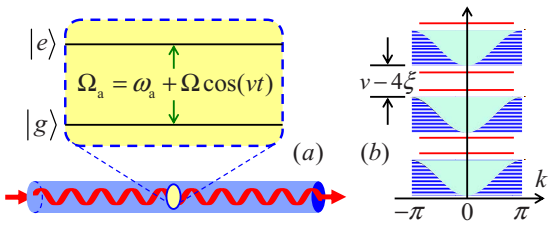

FIG. 1. (Color online) (a) Schematic diagram of a quantum switch: the coupled-resonator waveguide is coupled to a TLS with an energy-level spacing modulated by $\Omega_a(t)$. The Rabi oscillation can appear in the effective multiband structure of frequency shown in (b), with bound states (in red) in the gap.

$$H_C = \omega_c\sum_j a_j^\dagger a_j - \xi\sum_j (a_j^\dagger a_{j+1} + \text{H.c.}), \tag{6}$$

with the intercavity coupling constant ξ, which describes the photon moving from one cavity to another. For convenience, we take the zeroth cavity as the coordinate-axis origin and also assume that the TLS is located in this zeroth cavity. Under the rotating wave approximation, the interaction between the zeroth cavity field and the TLS is described by a Jaynes-Cummings Hamiltonian

$$H_I = \Omega_a(t)|e\rangle\langle e| + g(a_0^\dagger|g\rangle\langle e| + |e\rangle\langle g|a_0), \tag{7}$$

with coupling strength g and modulated transition frequency Ω_a of the TLS. By employing the Fourier transformation

$$a_j = \frac{1}{\sqrt{N}}\sum_k e^{ikj}a_k, \tag{8}$$

the second term in Eq. (7) and H_C can be rewritten in k space. In the rotating frame with respect to $H_C+\Omega_a(t)|e\rangle\langle e|$, the interaction Hamiltonian reads as

$$H_{II}(t) = \frac{g}{\sqrt{N}}\sum_{k;n} J_n\left(\frac{\Omega}{\nu}\right)[a_k^\dagger\sigma_- e^{i(\Delta-\epsilon_k-n\nu)t} + \text{H.c.}], \tag{9}$$

where we have used the Fourier-Bessel series identity. Here, the dispersion relation $\epsilon_k=2\xi\cos k$ describes an energy band of width 4ξ (the lattice constant l is assumed to be unity), $\sigma_-=|g\rangle\langle e|$. The $H_{II}(t)$ in Eq. (9) effectively describes a multiband Rabi oscillation.

In this work, we are mainly interested in the investigation of the transmission and localization of single photon in high-frequency regimes, corresponding to $\Delta, \xi \ll \nu$. For small ξ, compared with the modulation frequency ν, the gaps are

large and there is no energy-band overlap [the band structure is illustrated in Fig. 1(b)]. Otherwise, there exists a complex quantum dynamics with quantum chaos. In the high-frequency regime, the fast modulation in $\Omega_a(t)$ implies the resonance condition $n=0$. Therefore, the dynamic of the CRW+TLS is described by the effective Hamiltonian

$$H = H_C + \omega_a|e\rangle\langle e| + gJ_0\left(\frac{\Omega}{\nu}\right)(a_0^\dagger|g\rangle\langle e| + |e\rangle\langle g|a_0).$$

In the one excitation subspace, the wave function at arbitrary time

$$|\phi(t)\rangle = \sum_j u_j(t)e^{-i\omega_a t}|1_j g\rangle + u_e(t)e^{-i\omega_a t}|0e\rangle$$

is a superposition of the photon at the jth cavity with atom in the ground state and no photon in all cavities with atom in the excited state. The equations for the excited-state amplitude $u_e(t)$ and the amplitudes $u_j(t)$ of single-photon states derived from the Schroedinger equation with Hamiltonian H are given by

$$i\dot{u}_j(t) = \Delta u_j(t) - \xi[u_{j-1}(t) + u_{j+1}(t)] + Gu_e(t)\delta_{j0}, \quad (10a)$$

$$i\dot{u}_e(t) \simeq Gu_0(t), \quad (10b)$$

where the overdot indicates the derivative with respect to time. These amplitudes (10) show that the interaction between the single photon and the TLS is characterized by the effective *coupling* constant

$$G = gJ_0(\Omega/\nu).$$

For zeros of zeros of $J_0(\Omega/\nu)$, i.e.,

$$\Omega \cong 2.40\nu, 5.52\nu, \ldots,$$

the high-frequency modulation $\Omega_a(t)$ leads to the decoupling between the TLS and the CRW, and thus photons in the CRW will propagate freely without feeling the influence from the localized TLS. Therefore, this modulated TLS acts as a quantum "Zeno switch."

IV. FLOQUET-THEORY-BASED NUMERICAL SIMULATION OF THE DYNAMICAL QZE

Let us further study the QZE decoupling mechanism and the Zeno switch by numerically solving the time-dependent Hamiltonian H_C+H_I. Note that the total Hamiltonian is periodic in time, with period $2\pi/\nu$. Using Floquet theory, we define

$$H_F = H_C + H_I - i\partial_t, \quad (11)$$

as in, e.g., Ref. [29]. Each eigenstate $|f_n(t)\rangle$, with eigenvalue ε_n, of H_F can be used to define an eigenstate

$$|F_n\rangle = \exp(-i\varepsilon_n t)|f_n\rangle \quad (12)$$

of H_F with zero eigenvalue. Then the superposition of these eigenstates

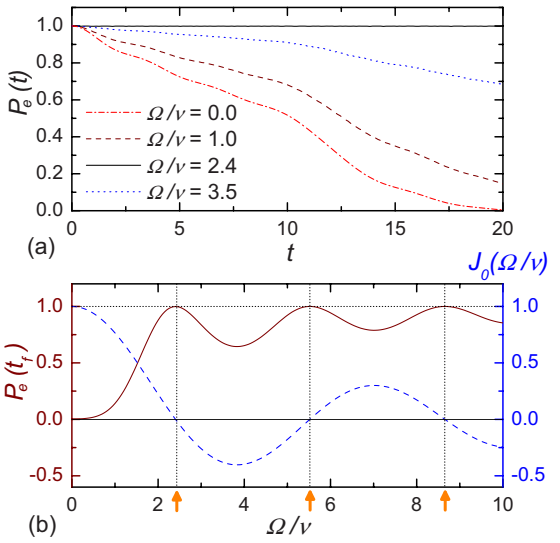

FIG. 2. (Color online) (a) Time dependence of the probability $P_e(t)$ for the TLS at its excited state with different Ω/ν, with parameters $\Delta=0$, $\xi=1.0$, $g=0.25$, $\nu=10$, and $L=41$ resonators; t is in units of $1/\xi$. Note that the excited state does not decay (i.e., QZE) when $\Omega/\nu=2.4$. (b) $P_e(t_f)$ (wine solid line) versus Ω/ν is plotted for a certain time $t_f=20$ using the same data as in (a). Obviously, the points for $P_e(t_f)=1$ (corresponding to no decay for the TLS) agree well with the zeros (orange vertical arrows) of $J_0(\Omega/\nu)$ (blue dashed line).

$$|\Phi(t)\rangle = \sum_n c_n|F_n\rangle \quad (13)$$

determines the general solution of the time-dependent Schrödinger equation corresponding to H_C+H_I. With an initial state $|\Phi(0)\rangle$, the coefficients c_n are given by

$$c_n = \langle f_n(0)|\Phi(0)\rangle.$$

Our task now is to diagonalize H_F in a discrete Hilbert space with the spatiotemporal basis vectors

$$|j;m_t\rangle = |j\rangle \otimes |m_t\rangle, \quad (14)$$

where m_t is the discrete temporal coordinate of the time t, satisfying

$$\langle t|m_t\rangle = \exp(i\nu m_t t)/\sqrt{T}, \quad (15)$$

with a large T; $|j\rangle$ is the eigenstate of the discrete space coordinate. On this time-varying basis $\{|j,m_t\rangle\}$, the matrix elements of H_F are independent of time.

For the dynamic QZE in this paper, the initial state $|\Phi(0)\rangle=|0,e;n_t=0\rangle$ evolves to $|\Phi(t)\rangle$. To keep the numerical accuracy and save computing time, we divide the total time t into N small time intervals τ, $t=N\tau$. In each interval, the system is evolved from $m\tau$ to $(m+1)\tau$. The final state of this interval becomes the initial state of the next interval. For a sufficiently small value of τ, an accurate wave function can be obtained, even when not too many $\{|m_t\rangle\}$ are used to represent H_F [29].

Figure 2(a) shows the probability $P_e(t)$ for the TLS to be in the excited state. When Ω/ν is tuned to the vicinity of the zeros of $J_0(x)$ (e.g., $\Omega/\nu=2.40$), the initially excited TLS

does not decay. Otherwise (e.g., $\Omega/\nu=0$, 1.0, 3.5), the probability $P_e(t)$ in the excited state decreases with time. Figure 2(b) shows how $P_e(t_f)$ varies with the ratio Ω/ν at the instant $t_f=20$ for $J_0(\Omega/\nu)$. It clearly demonstrates that the zeros of $J_0(\Omega/\nu)$ correspond to $P_e(t_f)=1$, i.e., the TLS does not decay. Thus, the numerical results agree well with our analytical results on the dynamical QZE.

V. QUANTUM ZENO DYNAMICS

In this section, we give the above-mentioned dynamic QZE a more standard approach in current literatures [31], which confirms the suitability for using the idea of QZE.

Within the subspace spanned by $|e0\rangle$ and $|gj\rangle$, if the TLS is prepared initially in the excited state, the evolution of the TLS-CRW system will lead to a superposition of states, corresponding to the TLS initially excited and no photons in the CRW and the TLS in the ground state and one photon in the CRW. The CRW forms a continuum. Therefore, the interaction process between the TLS and the CRW can be described in terms of a discrete level coupled to a continuum and will lead to a dissolution of the discrete state over an interval of width R, which is the decay rate of the discrete state to the continuum. A universal mechanism of quantum-mechanical decay control is usually based on periodic coherent pulses. This control can yield either the inhibition (Zeno effect) or the acceleration (anti-Zeno effect).

Following the analysis in Ref. [31], we calculate the probability

$$P_e(t) = \exp[-R(t)Q(t)] \tag{16}$$

to reflect the decay law (for detailed calculation, see the Appendix), where

$$Q(t) = \int_0^t d\tau |V(\tau)|^2 \tag{17}$$

is the effective interaction time with

$$V(t) = \exp\left[-i\frac{\Omega}{\nu}\sin(\nu t)\right] \tag{18}$$

here. In the frequency domain, the effective decay rate

$$R(t) = \int_{-\infty}^{\infty} \tilde{\Phi}(\omega+\Delta)F_t(\omega)d\omega \tag{19}$$

is the overlap of the normalized spectral modulation intensity

$$F_t(\omega) = \left|\int_0^t d\tau V(\tau)e^{-i\omega\tau}\right| / Q(t), \tag{20}$$

and the reservoir coupling spectrum $\tilde{\Phi}(\omega)$, which is the Fourier transformation of the memory function or reservoir response function

$$\Phi(t) = \frac{J^2}{N}\sum_k e^{i2\xi t\cos k}. \tag{21}$$

Obviously, $V(t)$ is periodic with the period ν^{-1}, the Bessel function $J_n(\Omega/\nu)$ of the first kind becomes the Fourier components of $V(t)$. At time t much larger than the period ν^{-1}, the decay rate reads as

$$R(t) = t\sum_{n=-\infty}^{+\infty} J_n^2\left(\frac{\Omega}{\nu}\right)\int_{-\infty}^{\infty}\tilde{\Phi}(\omega)\mathrm{sinc}^2\frac{(\omega-\Delta-n\nu)t}{2}d\omega, \tag{22}$$

where $\mathrm{sinc}\, x=\sin x/x$. Figure 2 roughly shows the dependence of the decay rate on the ratio of the driving amplitude to the driving frequency. As we mentioned before, we are interested in the high-frequency regime with parameters $\Delta, \xi \ll \nu$. Since the width of the reservoir spectrum is proportional to ξ, the relation of these parameters implies that the modulation frequency is much greater than the inverse correlation time of the continuum. Therefore, $\tilde{\Phi}(\omega)$ does not change significantly over the spectral intervals ν^{-1}. In this case, we can make the approximation

$$R(t) = tJ_0^2\left(\frac{\Omega}{\nu}\right)\mathrm{sinc}^2\frac{(\omega-\Delta)t}{2}\int_{-\infty}^{\infty}\tilde{\Phi}(\omega)d\omega. \tag{23}$$

The above equation describes that the state decays into all the channels of the reservoir. Since the effective decay rate is averaged over all decay channels [7], we work in the QZE regime. Obviously, the decay rate without modulation is suppressed by a factor $J_0^2(\Omega/\nu)$ when a periodical modulation is applied. When t is much larger than both ν^{-1} and an effective correlation time of the reservoir, one obtains

$$R(t) = J_0^2\left(\frac{\Omega}{\nu}\right)\tilde{\Phi}(\Delta), \tag{24}$$

i.e., the extension of the golden rule rate to the case of a time-dependent coupling [31]. Therefore, the atom remains in its initial state when the ratio between the modulation amplitude and the frequency meets the zeros of the Bessel function. We also note that when $A=0$, the zeroth Bessel function $J_0(0)=1$, which means the decay rate $R(t)=\tilde{\Phi}(\Delta)$ without any modulation.

VI. SCATTERED AND LOCALIZED PHOTONS WITH DYNAMICAL QZE

We now study the photon localization and the measurement on the QZE via photon scattering. The purpose for this study is twofold: (i) utilize the QZE-based mechanism to turn on or off the transmission of photons in the CRW, so that an ideal single-photon transistor can be realized and (ii) witness the dynamical QZE in the TLS by measuring the single-photon scattering. We further consider the relation between photon localization and the appearance of dynamic QZE.

Solutions to Eqs. (10) can be found in the form of either localized states around the location of the TLS or as a superposition of extended propagating Bloch waves incident reflected and transmitted by the TLS embedded in the CRW. It was done by first Fourier transforming the equations of motion of $u_j(t)$ and $u_e(t)$ in Eq. (10) to obtain their Fourier transforms $U_k(j)$ and $U_e(j)$,

$$E_k U_k(j) = \Delta U_k(j) - \xi[U_k(j-1) + U_k(j+1)] + G U_e \delta_{j0},$$

$$E_k U_e(j) = G U_k(j) \delta_{j0}. \quad (25)$$

Eliminating the amplitude $U_e(j)$ in the above equation, we obtain the discrete-coordinate scattering equation

$$[V(E_k) + \Delta - E_k] U_k(j) = \xi[U_k(j-1) + U_k(j+1)], \quad (26)$$

where

$$V(E_k) = g^2 J_0^2(\Omega/\nu)/E_k$$

is a resonant potential resulting from the second-order transition process due to the coupling with the TLS. It behaves as an infinite δ potential on the resonance $E_k=0$. In the absence of the TLS, a solution of Eqs. (10) has the form $U_k(j) = \exp(ikj)$, where k is the wave number of the Bloch waves. Therefore,

$$E_k = \Delta - 2\xi \cos k$$

gives a band of width 4ξ with its minimum lies at $k=0$. Within the band, the scattering wave function is assumed as

$$U_k(j) = \exp(ikj) + r \exp(-ikj), \quad (27)$$

for $j<0$, and

$$U_k(j) = s \exp(ikj),$$

for $j>0$, with the right- and left-moving waves $\exp(ikj)$ and $\exp(-ikj)$. The boundary conditions

$$U_k(0^+) = U_k(0^-), \quad (28a)$$

$$[V(E_k) + \Delta - E_k] U_k(0) = \xi[U_k(-1) + U_k(1)], \quad (28b)$$

result in the reflection amplitude $r=s-1$ and transmission amplitude

$$s = \frac{\omega_k - \omega_a}{\omega_k - \omega_a + i g^2 J_0^2(\Omega/\nu)/v_g}. \quad (29)$$

Here,

$$v_g = 2\xi \sin k$$

is the group velocity and

$$\omega_k = \omega_c - 2\xi \cos k$$

is the incident energy of the single photon.

Equation (29) indicates that when ω_a is inside the band ($\omega_k=\omega_c-2\xi\cos k$), a dip down to zero will occur in the transmission line shape $|s|^2$. This zero transmission is a *quantum interference* (Fano) effect characterized by certain discrete energy states interacting with the continuum. The *width* of the transmission line shape is determined by the ratio of the effective *coupling* strength $G=gJ_0(\Omega/\nu)$ to group velocity v_g. Obviously, the decoupling of the TLS-photon interaction occurs when $J_0(\Omega/\nu)$ vanishes. Consequently, the transmission dip disappears, i.e., the single photon goes through the TLS scatterer without absorption or emission. In other words, *by adjusting the amplitude and frequency of the modulating field* $\Omega_a(t)$*, the TLS spontaneous emission and stimulated transition are suppressed*. Measuring the photon transmission or reflection would show the occurrence of the dynamic QZE.

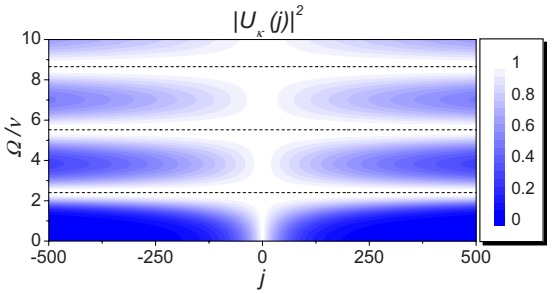

FIG. 3. (Color online) Contour plot of the square $|U_\kappa(j)|^2$ of the bound-state wave-function amplitude versus the ratio Ω/ν and the space coordinate j. The parameters here are the same as in Fig. 2. The horizontal dashed lines are the zeros of $J_0(x)$, corresponding to extended (along j) photon wave functions.

The CRW with the TLS embedded in can also support localized modes. We now discuss how to observe the dynamic QZE from the localization of photons described by the photonic bound state in the CRW. The bound state is assumed to have the following solutions with even parity for the eigenvalue (26):

$$U_\kappa(j) = (C \exp(-\kappa j), \ j > 0),$$

$$U_\kappa(j) = (C \exp(\kappa j), \ j < 0), \quad (30)$$

which is localized around the zeroth site, where the TLS is embedded. Here, the imaginary wave vector κ labels the energy

$$E_\kappa = \Delta \pm 2\xi \cosh \kappa \quad (31)$$

of a localized photon within the energy gap. The continuity of $U_\kappa(j)$ at the boundary $j=0$, i.e., Eq. (28) determines the existence condition of the bound state,

$$g^2 J_0^2\left(\frac{\Omega}{\nu}\right) = 2\xi(\xi \sinh 2\kappa \pm \Delta \sinh \kappa), \quad (32)$$

where the lower sign gives the living condition for the bound state, which lies upper the band with energy $E_\kappa=\Delta+2\xi\cosh\kappa$. On the resonance $\Delta=0$, the width of the bound state is determined by

$$\sinh 2\kappa = \frac{g^2 J_0^2(\Omega/\nu)}{2\xi^2}, \quad (33)$$

which can be adjusted by the ratio Ω/ν through $J_0(x)$. At the zeros of this Bessel function, $\kappa=0$ and the photon is delocalized. When off resonance, the energies of the two bound states are asymmetric with respect to the center of the band. In Fig. 3, we plot the single-photon distribution $|U_\kappa(j)|^2$ as a function of the discrete coordinate j, and the ratio Ω/ν. It shows that (1) the wave packet of the single photon spreads along the CRW as Ω/ν increases because

$$J_0 \sim x^{-1/2},$$

(2) the width of the localized photon state oscillates following $J_0(\Omega/\nu)$, (3) due to this modulation-induced Zeno effect,

the wave packet will be extended at the zeros of $J_0(x)$; (4) the full spreading of the photon wave packet does not occur as a periodic function of Ω/ν because the roots of $J_0(x)$ are not periodic. The above investigation indicates that the dynamic Zeno effect can be characterized by the delocalization of photons.

VII. CONCLUSION

Based on the dynamical QZE induced by a high-frequency modulation, we show how to decouple a TLS from its surroundings. We apply this QZE-based decoupling mechanism to realize a quantum switch for a photon. The dynamic QZE switch studied here allows to control the single-photon transport in a CRW by using a TLS, which is periodically modulated in time. Our analytical results agree well with our numerical results using Floquet theory. This proposal should be realizable experimentally [30] because the quantum Zeno switch only depends on the ratio between the amplitude Ω and the frequency ν of the external modulation. This QZE photon switch might be useful to quantum information science for the coherent control of single photons.

We note that if one puts atoms in a magneto-optical trap (MOT), with the atomic frequency modulated by the ac Stark effect, and observes the light scattering, complete reflection would not occur at the correct ratio of modulation strength to frequency, which is just like the one discussed here. However, due to the linear dispersion of the reservoir, which atoms in a MOT interact with, photon localization cannot be observed.

As we know that, in reality, all quantum systems interact with the environment, which results in the inelastic scattering of a single photon. The inelastic scattering of photons would reduce the transmission of photons as well as the quantum switching efficiency. The decoherence or dissipation either influences the free propagation of the single photon or broadens the width of the line shape at the resonance, according to its contributions to the scattering process. It is known that photon propagates freely in these resonators; all the dissipation factors of the resonators have an effect on the free propagation of the single photon. However, the decay of the two-level system influences the scattering process since the energy of photon is not conservative before and after its interacting with the two-level system; therefore, the width of the line shape is broadened.

ACKNOWLEDGMENTS

This work is supported by New Century Excellent Talents in University (Grant No. NCET-08–0682), NSFC Grants No. 10935010, No. 10474104, and No. 10704023, NFRPC Grants No. 2006CB921205 and No. 2007CB925204, and Scientific Research Fund of Hunan Provincial Education Department Grant No. 09B063. F.N. acknowledges partial support from the NSA, LPS, ARO, NSF Grant No. EIA-0130383, JSPS-RFBR Grant No. 06–02–91200, and the JSPS-CTC program. We thank S. Ashhab for useful discussions.

APPENDIX: QUANTUM ZENO DYNAMICS OF TWO-LEVEL SYSTEM IN AN ARTIFICIAL BATH

In this appendix, we follow Ref. [31] to discuss the quantum zeno dynamics of the two-level system in the CRW, which behaves as an artificial bath.

To this end, we make a Fourier transformation

$$\hat{a}_j = \frac{1}{\sqrt{N}} \sum_k e^{ikj} \hat{a}_k \tag{A1}$$

for Hamiltonian $H_C + H_I$ in Eqs. (6) and (7). In the subspace supported by the complete basis $\{|e0\rangle, |gk\rangle\}$, the Hamiltonian can be rewritten as

$$H = \sum_k \left[\omega_k |k\rangle\langle k| + \frac{J}{\sqrt{N}} |kg\rangle\langle 0e| + \text{H.c.} \right] + \Omega_a(t) |e\rangle\langle e|, \tag{A2}$$

where $\omega_k = \omega_c - 2\xi \cos k$. Therefore, the state at arbitrary time

$$|\phi(t)\rangle = \sum_j u_j(t) |1_j g\rangle + u_e(t) |0e\rangle \tag{A3}$$

lies within the subspace spanned by $|0e\rangle$ and $|kg\rangle$. Then, we obtain the equations for amplitudes u_k and u_e by substituting the state $|\phi(t)\rangle$ into the Schrödinger equation

$$i\partial_t U_k = \frac{J}{\sqrt{N}} U_e e^{-i(\omega_a - \omega_k)t} e^{-i(A/\nu)\sin(\nu t)},$$

$$i\partial_t U_e = \frac{J}{\sqrt{N}} \sum_k U_k e^{i(\omega_a - \omega_k)t} e^{i(A/\nu)\sin(\nu t)}, \tag{A4}$$

where the relation between the capital letter and the lowercase is given by

$$u_k = U_k e^{-i(\omega - 2\xi \cos k)t}, \quad u_e = U_e e^{-i[\omega_a t + (A/\nu)\sin(\nu t)]}. \tag{A5}$$

The above differential equations about U_k and U_e give an exact integro-differential equation for $U_e(t)$

$$\dot{U}_e = -\epsilon^*(t) \int_0^t d\tau U_e(\tau) \epsilon(\tau) \Phi(t-\tau) e^{i\Delta(t-\tau)}, \tag{A6}$$

where the detuning $\Delta = \omega_a - \omega_c$. Here

$$\Phi(t) = \frac{J^2}{N} \sum_k e^{i2\xi t \cos k} \tag{A7}$$

is the memory function or call reservoir response function, and the modulation function reads as

$$\epsilon(t) = e^{-i(A/\nu)\sin(\nu t)}. \tag{A8}$$

In the weak-coupling limit, the approximation $U_e(\tau) \approx U_e(t)$ can be made on the right-hand side of the Eq. (A6). Then we have

$$U_e(t) = \exp\left[-\int_0^t dt_1 \epsilon^*(t_1) \int_0^t dt_2 \epsilon(t_2) \Phi(t_1 - t_2) \times e^{i\Delta(t_1 - t_2)} \Theta(t_1 - t_2) \right]. \quad \text{(A9)}$$

The Fourier transformation of $\Phi(t)e^{i\Delta t}\Theta(t)$ is obtained

$$\tilde{\Phi}(\omega + \Delta)/2 = \frac{J^2}{2N} \sum_k \delta(\omega + \Delta + 2\xi \cos k),$$

which is expressed in terms of the coupling spectrum density $\tilde{\Phi}(\omega)$. The coupling spectrum is defined as the Fourier transformation of the reservoir response function

$$\tilde{\Phi}(\omega) = \frac{1}{2\pi} \int_{-\infty}^{\infty} \Phi(t) e^{i\omega t} dt. \quad \text{(A10)}$$

Further introducing the effective interaction time

$$Q(t) = \int_0^t d\tau |\epsilon(\tau)|^2 \quad \text{(A11)}$$

and defining the normalized spectral modulation intensity

$$F_t(\omega) = Q^{-1}(t) \int_0^t dt_1 \epsilon^*(t_1) e^{-i\omega t_1} \int_0^t dt_2 \epsilon(t_2) e^{i\omega t_2} = Q^{-1}(t) \left| \int_0^t dt' \epsilon(t') e^{i\omega t'} \right|^2,$$

the norm of amplitude reads as

$$|U_e(t)| = \exp\left[-\frac{Q(t)}{2} \int_{-\infty}^{\infty} \tilde{\Phi}(\omega + \Delta) F_t(\omega) d\omega \right].$$

The effective decay rate

$$R(t) = \int_{-\infty}^{\infty} \tilde{\Phi}(\omega + \Delta) F_t(\omega) d\omega \quad \text{(A12)}$$

is written as the overlap of the reservoir coupling spectrum and normalized spectral modulation intensity.

If the states $|k\rangle$ belong to a spectrally dense band, the CRW forms a "reservoir" spectral distribution $\tilde{\Phi}(\omega) = J^2 \rho(\omega)$, with spectral density given by

$$\rho(\omega) = \int_{-\pi}^{\pi} \delta(\omega + 2\xi \cos k) dk = \frac{1}{4} \int_{-\infty}^{\infty} e^{-i\omega x} J_0(2\xi x) dx = \begin{cases} 0, & 2\xi < |\nu - \omega| \\ \infty, & 2\xi = |\nu - \omega| \\ \dfrac{1/2}{\sqrt{4\xi^2 - \omega^2}}, & 2\xi > |\nu - \omega|. \end{cases}$$

$R(t)$ in Eq. (A12) was obtained by Kofman and Kurizki for very general cases to discuss the dynamics of Zeno and anti-Zeno effects in a heat bath. We only demonstrate their universal approach with our setup for coherent control of single-photon transfer. The detailed calculation for the decay rate begins with the effective interaction time $Q(t)=t$ and the modulation spectrum

$$F_t(\omega) = \sum_{n=-\infty}^{+\infty} J_n^2\left(\frac{\Omega}{\nu}\right) \text{sinc}^2\, \omega_n + \sum_{n_1 \neq n_2}^{+\infty} t J_{n_1}\left(\frac{\Omega}{\nu}\right) J_{n_2}\left(\frac{\Omega}{\nu}\right) \text{sinc}^2\, \omega_{n_1}\, \text{sinc}^2\, \omega_{n_2},$$

where $\omega_n = (\omega - n\nu)t/2$ and $\text{sinc}\, x = \sin x/x$. It yields the effective decay rate

$$R(t) = \sum_k \frac{tJ^2}{N} \left| \sum_{n=-\infty}^{+\infty} J_n\left(\frac{\Omega}{\nu}\right) \frac{\sin \dfrac{(\Delta + 2\xi \cos k + n\nu)t}{2}}{(\Delta + 2\xi \cos k + n\nu)t/2} \right|^2.$$

When no modulation is applied, i.e., $A=0$ and $t \to \infty$,

$$R(t) = 2\pi \tilde{\Phi}(\Delta),$$

which is the extension of the golden rule rate to the case of a time-dependent coupling. In this paper, we are interested in a regime with parameters $\Delta, \xi \ll \nu$, which means that the modulation frequency is much greater than the inverse correlation time of the continuum. The effective decay rate reads as

$$R(t) = \sum_k \frac{tJ^2}{N} \left| J_0\left(\frac{\Omega}{\nu}\right) \frac{\sin \dfrac{(\Delta + 2\xi \cos k)t}{2}}{(\Delta + 2\xi \cos k)t/2} \right|^2 = tJ_0^2\left(\frac{\Omega}{\nu}\right) \int_{-\infty}^{\infty} \tilde{\Phi}(\omega) \left| \frac{\sin \dfrac{(\omega - \Delta)t}{2}}{(\omega - \Delta)t/2} \right|^2 d\omega.$$

The above equation shows that the decay rate is determined by (1) the parameters of the driving field, i.e., ratio of modulation strength Ω to frequency ν; (2) the overlap the reservoir coupling spectrum and the modulation spectrum. Therefore, the width and the center of the spectrum are important factors. Obviously, the width of $\tilde{\Phi}(\omega)$ is less than 4ξ; the center of $\tilde{\Phi}(\omega)$ lies in $\omega_M^G = 0$. The width of $F_t(\omega)$ is t^{-1}, Δ is its center. This following results can be obtained. (1) If the ratio of modulation strength Ω to frequency ν satisfies $J_0(\Omega/\nu) = 0$, then the effective decay rate $R(t)=0$. (2) For sufficiently long times, i.e., t is much larger than both ν^{-1} and an effective correlation time $(4\xi)^{-1}$, the decay rate

$$R(t) = J_0^2\left(\frac{\Omega}{\nu}\right) \tilde{\Phi}(\Delta). \quad \text{(A13)}$$

(3) When time $t \sim \nu^{-1}$, with $\nu \gg \Delta, 2\xi$, the normalized spectral modulation intensity is a small varying function over the interval 4ξ; therefore, one can make the approximation

$$R(t) = tJ_0^2\left(\frac{\Omega}{\nu}\right) \text{sinc}^2 \frac{(\omega - \Delta)t}{2} \int_{-\infty}^{\infty} \tilde{\Phi}(\omega) d\omega.$$

Since the effective decay rate is averaged over all decay channels, the quantum Zeno effect generally occurs.

[1] B. Misra and E. C. G. Sudarshan, J. Math. Phys. **18**, 756 (1977).
[2] K. Koshino and A. Shimizu, Phys. Rep. **412**, 191 (2005).
[3] D. Home and M. A. B. Whitaker, Ann. Phys. **258**, 237 (1997).
[4] J. D. Franson, B. C. Jacobs, and T. B. Pittman, Phys. Rev. A **70**, 062302 (2004).
[5] X. B. Wang, J. Q. You, and F. Nori, Phys. Rev. A **77**, 062339 (2008).
[6] Y. P. Huang and M. G. Moore, Phys. Rev. A **77**, 062332 (2008).
[7] A. G. Kofman and G. Kurizki, Nature (London) **405**, 546 (2000).
[8] L. Zhou, F. M. Hu, J. Lu, and C. P. Sun, Phys. Rev. A **74**, 032102 (2006).
[9] A. Peres, Am. J. Phys. **48**, 931 (1980).
[10] T. Petrosky, S. Tasaki, and I. Prigogine, Physica A **170**, 306 (1991); Phys. Lett. A **151**, 109 (1990).
[11] L. E. Ballentine, Phys. Rev. A **43**, 5165 (1991).
[12] E. Block and P. R. Berman, Phys. Rev. A **44**, 1466 (1991); C. Search and P. R. Berman, Phys. Rev. Lett. **85**, 2272 (2000); Phys. Rev. A **62**, 053405 (2000).
[13] C. P. Sun, X. X. Yi, and X. J. Liu, Fortschr. Phys. **43**, 585 (1995).
[14] L. Viola and S. Lloyd, Phys. Rev. A **58**, 2733 (1998).
[15] P. Facchi, D. A. Lidar, and S. Pascazio, Phys. Rev. A **69**, 032314 (2004).
[16] W. M. Itano, D. J. Heinzen, J. J. Bollinger, and D. J. Wineland, Phys. Rev. A **41**, 2295 (1990).
[17] M. C. Fischer, B. Gutierrez-Medina, and M. G. Raizen, Phys. Rev. Lett. **87**, 040402 (2001).
[18] E. W. Streed, J. Mun, M. Boyd, G. K. Campbell, P. Medley, W. Ketterle, and D. E. Pritchard, Phys. Rev. Lett. **97**, 260402 (2006).
[19] C. P. Sun, L. F. Wei, Y. X. Liu, and F. Nori, Phys. Rev. A **73**, 022318 (2006); M. Mariantoni, F. Deppe, A. Marx, R. Gross, F. K. Wilhelm, and E. Solano, Phys. Rev. B **78**, 104508 (2008).
[20] J. T. Shen and S. Fan, Phys. Rev. Lett. **95**, 213001 (2005); **98**, 153003 (2007); Opt. Lett. **30**, 2001 (2005).
[21] L. Zhou, Z. R. Gong, Y. X. Liu, C. P. Sun, and F. Nori, Phys. Rev. Lett. **101**, 100501 (2008).
[22] D. E. Chang, A. S. Søensen, E. A. Demler, and M. D. Lukin, Nat. Phys. **3**, 807 (2007).
[23] J. Kim, O. Benson, H. Kan, and Y. Yamamoto, Nature (London) **397**, 500 (1999).
[24] P. Bermel, A. Rodriguez, S. G. Johnson, J. D. Joannopoulos, and M. Soljačić, Phys. Rev. A **74**, 043818 (2006).
[25] B. Dayan, A. S. Parkins, T. Aoki, E. P. Ostby, K. J. Vahala, and H. J. Kimble, Science **319**, 1062 (2008).
[26] F. Y. Hong and S. J. Xiong, Phys. Rev. A **78**, 013812 (2008).
[27] A. Faraon, I. Fushman, D. Englund, N. Stoltz, P. Petroff, and J. Vučković, Nat. Phys. **4**, 859 (2008).
[28] S. Ashhab, J. R. Johansson, A. M. Zagoskin, and F. Nori, Phys. Rev. A **75**, 063414 (2007).
[29] U. Peskin and N. Moiseyev, J. Chem. Phys. **99**, 4590 (1993).
[30] J. Q. You and F. Nori, Phys. Today **58**(11), 42 (2005).
[31] A. G. Kofman and G. Kurizki, Phys. Rev. Lett. **87**, 270405 (2001)